CrossMark

Analysis of hydrological extremes at different hydro-climatic regimes under present and future conditions

I. G. Pechlivanidis [1] · B. Arheimer [1] · C. Donnelly [1] ·
Y. Hundecha [1] · S. Huang [2] · V. Aich [2] · L. Samaniego [3] ·
S. Eisner [4] · P. Shi [5]

Abstract We investigate simulated hydrological extremes (i.e., high and low flows) under the present and future climatic conditions for five river basins worldwide: the Ganges, Lena, Niger, Rhine, and Tagus. Future projections are based on five GCMs and four emission scenarios. We analyse results from the HYPE, mHM, SWIM, VIC and WaterGAP3 hydrological models calibrated and validated to simulate each river. The use of different impact models and future projections allows for an assessment of the uncertainty of future impacts. The analysis of extremes is conducted for four different time horizons: reference (1981–2010), early-century (2006–2035), mid-century (2036–2065) and end-century (2070–2099). In addition, Sen's non-parametric estimator of slope is used to calculate the magnitude of trend in extremes, whose statistical significance is assessed by the Mann–Kendall test. Overall, the impact of climate change is more severe at the end of the century and particularly in dry regions. High flows are generally sensitive to changes in precipitation, however sensitivity varies between the basins. Finally, results show that conclusions in climate change impact

This article is part of a Special Issue on " Hydrological Model Intercomparison for Climate Impact Assessment" edited by Valentina Krysanova and Fred Hattermann.

Electronic supplementary material The online version of this article (doi:10.1007/s10584-016-1723-0) contains supplementary material, which is available to authorized users.

✉ I. G. Pechlivanidis
  ilias.pechlivanidis@smhi.se

[1] Swedish Meteorological and Hydrological Institute, Norrköping, Sweden

[2] Potsdam Institute for Climate Impact Research, Potsdam, Germany

[3] Helmholtz Centre for Environmental Research – UFZ, Leipzig, Germany

[4] Center for Environmental Systems Research, University of Kassel, Kassel, Germany

[5] Center for Global Change and Water Cycle, Hohai University, Nanjing, China

studies can be highly influenced by uncertainty both in the climate and impact models, whilst the sensitivity to climate modelling uncertainty becoming greater than hydrological model uncertainty in the dry regions.

1 Introduction

The increase in the atmospheric concentrations of greenhouse gases has led to the global climate change phenomenon which is expected to have a strong impact on water resources at local, regional and global scales (IPCC 2013). Commonly the modelling chain for climate change impact assessment involves climate variables from global climate models (GCMs), which for hydrological modelling purposes are dynamically downscaled using regional climate models (RCM) to represent local basin-scale features and dynamics (Fowler et al. 2007); however, there are investigations in which GCMs are used directly in hydrological modeling (Todd et al. 2011). However, due to the inherent remaining bias of GCM/RCM output, bias correction methods are applied to render the GCM/RCM data useful for hydrological impact modelling (Christensen et al. 2004; Chen et al. 2012).

Projecting climate impacts on hydrological processes is often prone to considerable uncertainties (i.e. from greenhouse gas emission scenarios, climate models and their parameterisation, downscaling techniques, bias correction methods, hydrological models structure and parameters), which are unavoidably propagated through the entire modeling chain and further interact with each other (Minville et al. 2008; Refsgaard et al. 2010). These uncertainties can propagate in a very complex way (e.g. magnitude of error could vary both in space and time), which could be misinformative for management decisions. An increasing interest has therefore been shown to quantify the contribution from each uncertainty source to the total uncertainty (Preston and Jones 2008; Poulin et al. 2011; Teutschbein and Seibert 2012).

In the modelling chain, future emission scenarios, described by the representative concentration pathways (RCP), are the first source of uncertainty. Hawkins and Sutton (2009) showed that towards the end of the twenty-first century, the RCPs are the dominant source of uncertainty in climate projections. In regard of the climate models, also the choice of GCM and RCM can have a large impact on the results and generally an ensemble of projections – encompassing different GCMs, RCMs and emission scenarios – is recommended in hydrological climate change impact assessment (Hewitt and Griggs 2004; Collins 2007). A clear distinction on the relative effects of hydrological model (HM) uncertainty and climate model (CM) uncertainty to the projected discharge uncertainty has not been concluded; results vary between studies depending on catchment climate and hydrological variable studied (Hagemann et al. 2013; Velázquez et al. 2013; Vetter et al. 2015). However, the impact of HM structural uncertainty on projected discharge changes can be significant due to, for instance, the differences in the representation of evapotranspiration and snow/ice accumulation/melting processes (Poulin et al. 2011; Viviroli et al. 2011).

A large effort has been given to assessing climate change impacts on hydrological processes, mostly focusing on long-term means, seasonal and/or monthly water resources, i.e. discharge, runoff, soil moisture (Chiew et al. 2009; Buytaert and De Bièvre 2012). However, it is apparent that the changes in hydrological extremes, i.e. floods and droughts, would have more profound and immediate impacts on agriculture, economy, and human health than the seasonal or monthly changes (Arnell 2011; Taye et al. 2011). Changes in hydrological extremes are expected to vary between basins. For instance, basins in which flood events are

driven by snow melting may experience a change in their response if climate change affects winter and spring temperatures that lead to losses of the snowpack before the onset of the spring melt (Burn et al. 2010). Similar types of changes can be expected for low flows, with climate change affecting their magnitude and seasonality (Demirel et al. 2013).

Conventionally hydrological impacts on large river basins have been studied within global or continental impact studies; however large-scale studies entail compromises in model input data and calibration at the local scale (occasionally not being possible) (Donnelly et al. 2014; Arheimer and Lindström 2015). Analysing climate change impacts between different regions in individually calibrated models allows for a comparative analysis and a holistic overview of the potential impacts, and can inform on the uncertainties in previous continental/global scale studies (e.g. Prudhomme et al. 2014; Roudier et al. 2015). Nevertheless, it is not clear whether a calibrated regional model is more trustworthy in terms of climate change projections than a global/continental model (which is uncalibrated and performs worse at a particular site in the historical period), and needs further investigation.

The objectives of this article are: i) to detect trends in hydrological extremes (high and lows flows) as climate changes in five large basins with differing climatic conditions, ii) to identify the impact of climate change on hydrological extremes, iii) to quantify the differences in the sensitivity of high flows on climate between the basins, and iv) to estimate the modelled uncertainty and its potential relation to the basin's climatic conditions. To achieve these objectives, we analyse the results from the Inter-Sectoral Impact Model Intercomparison Project phase 2 (ISI-MIP2), which, in this investigation, consists of future hydrological projections based on five regional-scale hydrological models, driven by five GCMs and four RCPs (available from ISI-MIP phase 1; ISI-MIP) for five large basins in three continents.

2 Study areas and data

2.1 Study areas

Five basins from three continents were selected from the set of 12 basins within ISI-MIP2, including two basins in Europe (the Rhine River at the Lobith station, and Tagus at Almourol), one in Africa (Niger at Lokoja), and two in Asia (Ganges at Farakka, and Lena at Stolb). The basin selection was based on the regional/modelling interests of the first author, however the basins span a wide hydro-climatic gradient from dry to wet systems. The location as well as the physical and hydro-climatic characteristics of these basins can be found in Fig. 1 and Table 1 in the introductory paper by Krysanova and Hattermann (this special issue); to avoid redundant information we do not repeat them here.

2.2 Atmospheric forcing and climate projections

The WATCH Forcing Data (Weedon et al. 2011) are used to provide daily precipitation, mean-minimum-maximum temperature, air humidity, solar radiation and wind speed inputs for the period 1971–2001 at 0.5° resolution. In brief, the WATCH data are derived based on a combination of the ERA-40, the 40-year reanalysis of the European Centre for Medium Range Weather Forecasts (ECMWF) and the Climate Research Unit TS2.1 dataset (CRU). For future predictions, the ensemble of 20 climate projections consists of

modelling chains that use five GCMs from the CMIP5 archive (HadGEM2-ES, IPSL-5 CM5A-LR, MIROC-ESM-CHEM, GFDL-ESM2M, and NorESM1-M, here abbreviated as Hadley, IPSL, MIROC, GFDL, and Nor respectively) and four different RCPs. RCPs are numbered after their increased radiative forcing until year 2100 (+2.6, +4.5, +6.0 and +8.5 W/m^2, respectively). The projections were bias corrected against the WATCH dataset (see details in Hempel et al. 2013) and are available at 0.5° resolution. The projections cover the period from 1st Jan. 1950 to 31st Dec. 2099, and are available from ISI-MIP. The current analysis is based on four 30-year periods from the bias-corrected climate projections: reference (1981–2010), early-century (2006–2035), mid-century (2036–2065), and end-century (2070–2099) period.

3 Methodology

3.1 Hydrological impact models

Five process-based hydrological models participated in this study: HYPE, mHM, SWIM, VIC and WaterGAP3. In contrast to previous ISI-MIP studies where global hydrological models were used (Davie et al. 2013), models were set up, calibrated and validated individually for each basin. Out of the five selected basins, modelled data from the mHM model are only available for the Rhine and Ganges River basins. References and information about the model set-ups are listed in the introductory paper by Krysanova and Hattermann. VIC, WaterGAP3 and mHM perform their simulations on a regular lat-lon grid. HYPE and SWIM disaggregate a river basin into subbasins and hydrotopes (hydrological response units) of irregular shape. Evapotranspiration is computed based on different algorithms (and hence requires different parameters) depending on the impact models (see Table 3 in Krysanova and Hattermann, this special issue). The models also differ in complexity, storage and runoff generation mechanisms, and routing. Further details about the models can be found in Krysanova and Hattermann (this special issue).

All models are calibrated and validated following the ISI-MIP protocol, which defines the targeted flow stations. Although anthropogenic activities can alter the flow dynamics at the regional scale, their impact at the basin outlets, in which this analysis is based, is usually not so large due to the smoothing/delaying effect occurring at this large scale. The water management was not included in most of model applications in this study (except SWIM for Tagus and HYPE), but it is planned to be included in the coming experiments. A good performance in terms of long-term means, moderate and high flows, variability and dynamics, is achieved by most models, yet the performance for low flows is quite poor in many cases (see Huang et al., this special issue).

3.2 Climate change impact assessment

Here, we investigate extreme values of discharge, i.e. high and low flows. We therefore investigate three percentiles of flow, i.e. 10th, 90th and 99th (named as Q_{90}, Q_{10} and Q_{01}), which are robust indicators for low and (very) high flows. A positive (negative) trend in Q_{10} and Q_{01} means an increase (reduction) in flood hazard, with Q_{01} being more informative for more extreme hazards. A negative trend in Q_{90} implies a further reduction in low flows, potentially leading to more severe and/or frequent hydrological droughts.

3.2.1 Trend analysis

The non-parametric Mann-Kendall (MK) test is used to statistically assess the existence of monotonic linear or non-linear trends of annual very high (Q_{01}) and low (Q_{90}) flows over time (1981–2099) (Mann 1945). MK is a statistical test widely used for the analysis of trends in climatological and in hydrological time series. Due to its non-parametric nature, the method does not require the data to be normally distributed, whilst the test has low sensitivity to abrupt breaks due to inhomogeneous time series. The MK test was used with a 5 % significance level.

If a trend is present in the data, then the slope (change per unit time) is estimated using a simple nonparametric procedure developed by Sen (1968). In here, the Sen's slope (also known as the Kendall slope) is a linear trend, which is the median trend of the time series. Sen's slope is an unbiased estimator of the true slope (unbiased to outliers) and can be more accurate than non-robust simple linear regression for skewed and heteroskedastic data.

3.2.2 Long-term averages

We next assess the impact of climate change on high and low flows over periods of interest, represented by the 90th and 10th percentiles of flow, respectively, in each basin. The daily flow series for each 30-year period (reference, early-, mid- and end-century) are used to extract the statistics. The relative future change in the long-term average (%) between two periods (early-, mid- or end-century versus reference period) due to climate change is estimated for each basin. Positive change indicates an increase of the corresponding value in the reference period.

3.3 Sensitivities and uncertainties

3.3.1 Discharge-climate sensitivity

We further investigate the sensitivity of the projected high flows (Q_{10}) and low flows (Q_{90}) to precipitation (P_{mean}; annual mean of precipitation). The relative changes (anomalies) of the annual Q_{10}, Q_{90} and P_{mean} values for each year of the period 2006–2099 compared to the means of the reference period of the same scenario are calculated, and the Q_{10} to P_{mean} and Q_{90} to P_{mean} relations are analysed.

3.3.2 Decomposing climate - impact model uncertainties

We finally decompose the total Q_{10} and Q_{90} modelled uncertainty into the two main sources, i.e. CM uncertainty and HM uncertainty. To quantify the uncertainty propagated due to CM (HM) uncertainty, we focus on a single HM (GCM) and quantify the variability, here represented by the standard deviation, in the future changes in Q_{10} and Q_{90} from all GCMs (HM). This is repeated for each HM (GCM) and the mean of all the standard deviations describes the uncertainty from the CM (HM). We then investigate potential links between CM and HM uncertainties to the regional climatic conditions using the Budyko diagram (curve). The diagram relates a metric of the mean annual water balance (ratio of mean annual evaporation to mean annual precipitation) to a climatic aridity index (mean annual potential evaporation to mean annual precipitation). The location of a basin in the Budyko curve

represents the relative degree of water versus energy limitation and can inform the coarse interpretation of the controls on basin response (Blöschl et al. 2013).

4 Results and discussion

4.1 Trend analysis

The trends in the annual Q_{01} and Q_{90} data for three periods (from 1981 up to the end of early-, mid-, and end-century) are analysed for each impact model and driving GCM for all five basins and two RCP scenarios (RCP2.6 and 8.5 representing a mild and an extreme emission scenario) (Fig. 1). Overall, the direction of Q_{01} trends lack statistical significance except the identified end-century trends (and mid-century for the Lena basin), particularly for RCP8.5, while Q_{90} trends are significant for most basins for the mid- and end-century, particularly for RCP8.5 (only Lena shows significant trends for the mid-century for RCP2.6). It is important to note that for a given impact model the direction of future trends varies depending on the driving CM (as expected); however for a given climate model, the direction of trends from the impact models is consistent. Moreover, for Q_{01} and for some CM-HM combinations (e.g. for the Ganges, Lena and Niger basins under RCP2.6), the trends appear to be stronger for the early-century compared to the end-century, yet they tend to be significant only for the later periods. This temporal variability in the flow trends is subject to effects of joint precipitation and temperature temporal changes.

Overall, an increasing trend in high and low flows is shown for the Lena basin (increasing in significance with increasing emissions scenarios and future period; for Q_{90} the significance is increased with increasing future period only for RCP8.5) but in the Rhine basin only for the end-century for RCP2.6. For the Ganges basin an increasing trend is shown only for high
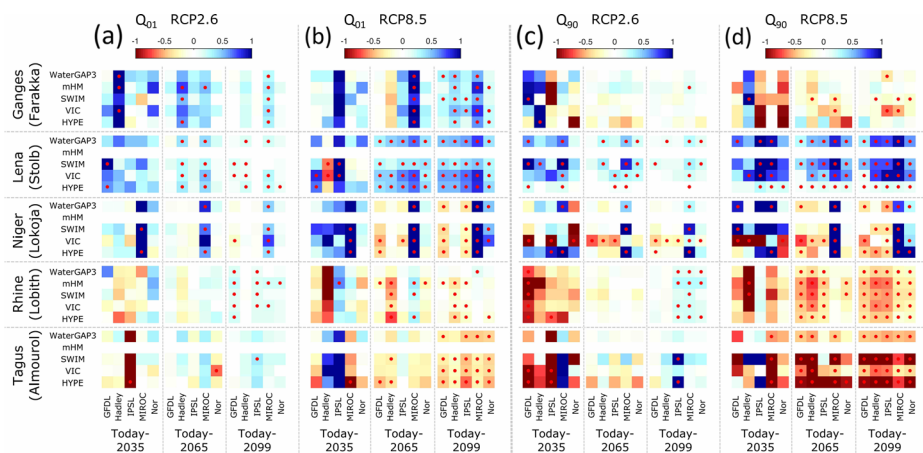

Fig. 1 Trends in Q_{01} (**a-b**) and Q_{90} (**c-d**) at the five basins during the three future scenario periods for RCP2.6 and RCP8.5. Results are for all five basins, five GCMs and five impact models (note that results for the mHM model are only available for the Rhine and Ganges River basins). Boxes with a red dot indicate statistical significance (5 % significance level) based on the MK test

flows; yet the strength is not increased. Decreasing trends in high and low flows are shown for the Rhine and Tagus under RCP8.5 for the mid- and end-century, while the pattern of trends for the Niger is highly uncertain. Although statistically significant trends are projected for the Niger River basin for the end-century for both RCP2.6 and 8.5, the trends for the latter show an alternation of positive (quite strong) and negative slopes depending on the GCM scenario. Again, this highlights the presence of uncertainty in the future climate projections. Of particular interest is the alternation from positive (although not statistically significant) to negative trend during the early- and end-century. This could be due to the temporal patterns of the climatic variables in the Niger basin and was also found with a different set of RCMs by Aich et al. (2015).

4.2 Changes in long-term means

Results for changes in Q_{10} and Q_{90} are presented in Figs. 2 and 3 for all five basins, four RCPs and three future periods. The relative difference in changes depends on the emission scenario, basin, and future period; however, in general, changes in Q_{10} and Q_{90} vary within similar ranges (as Figs. 2 and 3 show between −50 and 200 %), with the Ganges basin being an exception since changes in Q_{10} seem to be more significant than changes in Q_{90} in the mid- and end-century.

As shown by most of the model combinations, Q_{10} in the Ganges and Lena is expected to increase, while Q_{10} is generally shown to decrease in the Tagus. Results for the Rhine and Niger basins are uncertain with the potential changes being dependent on the CM. In particular, in the Ganges, Q_{10} is shown to increase by up to ~100 % at the end of the century. Although projected changes in the Ganges are largely variable between the driving GCM models, the direction of change is consistent between the HMs for a given GCM model. Consistently across projections, the
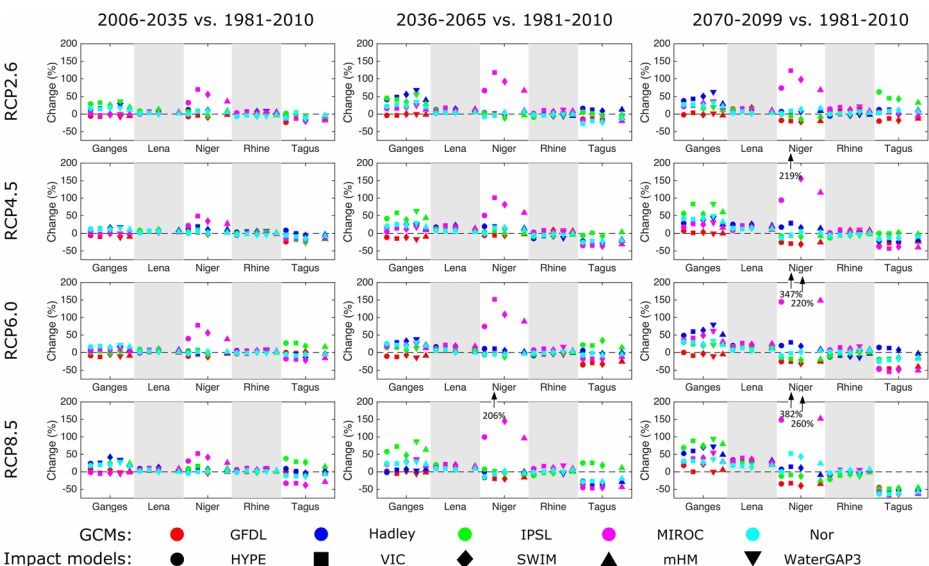

Fig. 2 Percentage change in Q_{10} at five basins in the three future scenario periods compared to the reference period (1981–2010). Results correspond to the five GCMs, five impact models, and four RCP scenarios
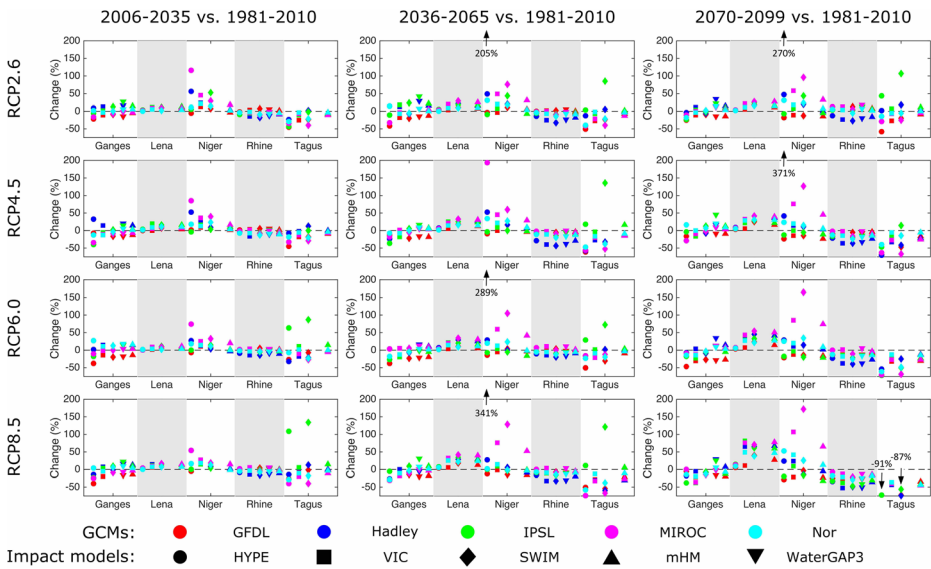
Fig. 3 Percentage change in Q_{90} at five basins in the three future scenario periods compared to the reference period (1981–2010). Results correspond to the five GCMs, five impact models, and four RCP scenarios

Lena basin high flows are shown to slightly increase with increases of up to ~40 % at the end of the century. Lena's flow regime is strongly influenced by snow/ice accumulation/melting processes, which within the HM context are heavily controlled by temperature. It is therefore expected that, given also the increase in precipitation, the temporal distribution of temperature has a major impact on this result. Conclusions are supported by the changes in the monthly Q_{10} values; see the impacts on seasonality for all basins and models in Fig. S1 in the Supplement.

For the Niger, results are highly variable with for example the MIROC-driven outputs projecting increases in Q_{10} from 100 to 300 %. A similar range in Q_{10} change for this basin was observed by Aich et al. (2014). The discrepancies between CM-driven results are amplified in the end-century; however, the MIROC-driven outputs are highly variable even between the impact models. This could be due to HM structural inability to represent the processes in the floodplain of the Inner Niger Delta, which has a remarkable impact on the flow regime (about 40 % of the inflowing water evaporates from the floodplain). The Rhine basin shows the smallest expected changes in high flows (between ~ ±15 %) in all RCPs and future periods. As expected, the projected changes are larger for RCP8.5 compared to other RCPs, but still smaller in comparison to the changes shown in the other basins. In the Tagus basin, for higher end emissions scenarios (RCP4.5 to 8.5), a reduction in Q_{10} is projected for the end-century following the general reduction in precipitation over the region. The pattern is more complicated in the early-century with some driving models projecting increases (IPSL and Hadley) and others projecting reductions.

For low flows, changes related to the different HMs and driving CMs seem to be highly variable. Overall, an increase in Q_{90} is projected for the Lena (all CM-HM combinations) and Niger basins (apart from the GFDL-driven and some cases of the IPSL-driven results in the mid- and end-century), while a reduction is shown for the Rhine (apart from very few CM-HM combinations in the end-century) and Tagus (apart from cases of the IPSL-driven results).

Results for the Ganges are uncertain, yet most CM-HM combinations show a reduction for RCP8.5 (up to ~ −50 %).

In particular, the Ganges results seem to be more dependent on the HM, RCP and future period than CM. On the contrary, results for the snowmelt dominated Lena basin show a consistent increase in low flows (increasing in significance with increasing emission scenarios and future period). In the Niger basin, increased Q_{90} seems to be expected due to the increase in precipitation (between 5.3 and 12.2 % in the early- and mid-century according to Krysanova and Hattermann, this special issue). However, the variability between future changes is very high for the end-century. In the Rhine basin, the reduction in Q_{90} (up to −50 % in the end-century) seems to occur due to the joint effect of temperature and precipitation; a high increase in temperature (between 0.9 and 4.4 °C) and a relatively minor increase in precipitation (between 1 and 6.6 %); see Krysanova and Hattermann (this special issue). In the Tagus basin, most of the model runs indicate a reduction in Q_{90} of up to −50 % following the projected decrease in precipitation (between −0.9 and −27.3 %). Notable exceptions are the IPSL-driven projections that indicate an increase for some impact models, RCPs and future periods.

4.3 Climate sensitivity

Figure 4 illustrates the Q_{10}, Q_{90} anomalies plotted against P_{mean} anomalies for each year of the period 2006–2099 under RCP8.5. An increase in precipitation results in an increase in high and low flows; however this relationship is not linear and its strength varies between the basins in accordance to their runoff coefficient (Table 1 in the introductory paper by Krysanova and Hattermann). The Q_{10} to P_{mean} and Q_{90} to P_{mean} sensitivities vary significantly between basins with the Niger's response being the most sensitive to precipitation. Results for the Niger show that an increase (reduction) of 25 % in precipitation will result in ~60 % increase (~ 50 % reduction) on average in Q_{10}. Results for the Niger are particularly interesting with the Q_{10} to P_{mean} and Q_{90} to P_{mean} anomalies being clustered since the MIROC-driven results are different from the other GCM-driven results. This highlights how different the sensitivity of the results is to different CMs.

In the Lena basin, an increase (reduction) of 25 % in annual precipitation results in an ~30 % and 45 % increase (~ 25 % and 20 % reduction) on average of Q_{10} and Q_{90} respectively. As mentioned in Section 4.2, snow/ice accumulation/melting (which are heavily controlled by temperature) strongly affects the flow regime in this basin. A similar sensitivity to climate is observed for Q_{10} in the Rhine basin. The strength of the relationship is slightly lower than that for the Niger (yet adjusted $R^2 \geq 0.25$ (which indicates an acceptable degree of predictability) only for Q_{10}), however the response to a 25 % increased annual precipitation is a 30 % increase in Q_{10}. For the Ganges and Tagus an increase in mean precipitation of 25 % results in increases in Q_{10} of 50 and 35 %, respectively. However the Q_{10} to P_{mean} and Q_{90} to P_{mean} trends are not statistically significant (based on the adjusted R^2 value). Uncertainties from the GCMs and impact models seem to mask these relationships, and therefore caution is needed regarding the interpretation of these results.

The analysis for high flows was repeated using the 90th percentile of precipitation (P_{10}) instead of P_{mean} (Fig. S2 in the Supplement). The results were very similar to those above, however the strength of the relationships was slightly lower (slightly smaller adjusted R^2 values), and hence conclusions remain the same.
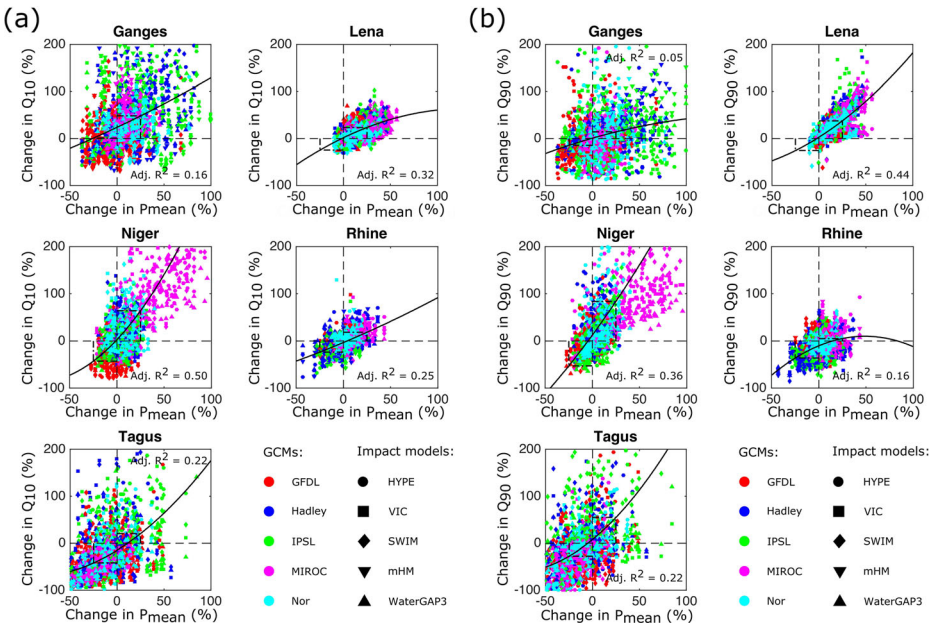
Fig. 4 Climate sensitivity of the (**a**) Q_{10} and (**b**) Q_{90} for the five basins: change in modelled annual Q_{10} and Q_{90} discharge per change of P_{mean} precipitation for the years 2006–2099 compared to the mean of base period 1981–2010 for five GCMs in RCP8.5. Curve shows fitted local regression (polynomial) over all values, together with the adjusted R^2 values (adjusted R^2 explains the proportion of the variation in a dependent variable explained by more than one independent variables for a linear regression model)

4.4 Uncertainty in future projections

Figure 5 analyses uncertainty in future projections, as this can be decomposed into uncertainty from the driving CMs and HMs, and related to the basins' climatic conditions for RCP2.6 and 8.5 (see explanation in Section 3.3). The basins are ranked based on their dryness and evaporative indices. The Niger basin has the warmest climate and hence the highest dryness index, followed by the Ganges and Tagus. The dryness indices are almost similar for the Rhine and Lena basins. Figure 5 shows that uncertainty (described by the mean standard deviation of Q_{10} and Q_{90} change) propagated from both CMs and HMs generally increases under increasingly dry climatic conditions. This is particularly emphasised for RCP8.5. The increase of uncertainties under dry conditions is related to the quantification of actual evapotranspiration, which is a dominant flux in such environments. The HMs have applied different algorithms for potential and actual evapotranspiration to close the water balance (see Table 3 in Krysanova and Hattermann, this special issue), yet there is still incomplete understanding of how much water is lost via evaporation and/or transpiration to the atmosphere, and hence increased uncertainty is related to that..

Starting for high flows, in the wetter regions (Lena and Rhine basins), the propagated uncertainty from CMs and HMs is of similar magnitude (standard deviation of change is ~10 % in both model sets). However, CM uncertainty dominates the spread in the projections of discharge in the dry regions. In the Ganges basin under both RCP2.6 and 8.5, CM uncertainty is three times higher than the uncertainty propagated from HMs; the standard deviation of Q_{10} change due to climate modelling is ~28 % for RCP8.5. In the Niger basin,
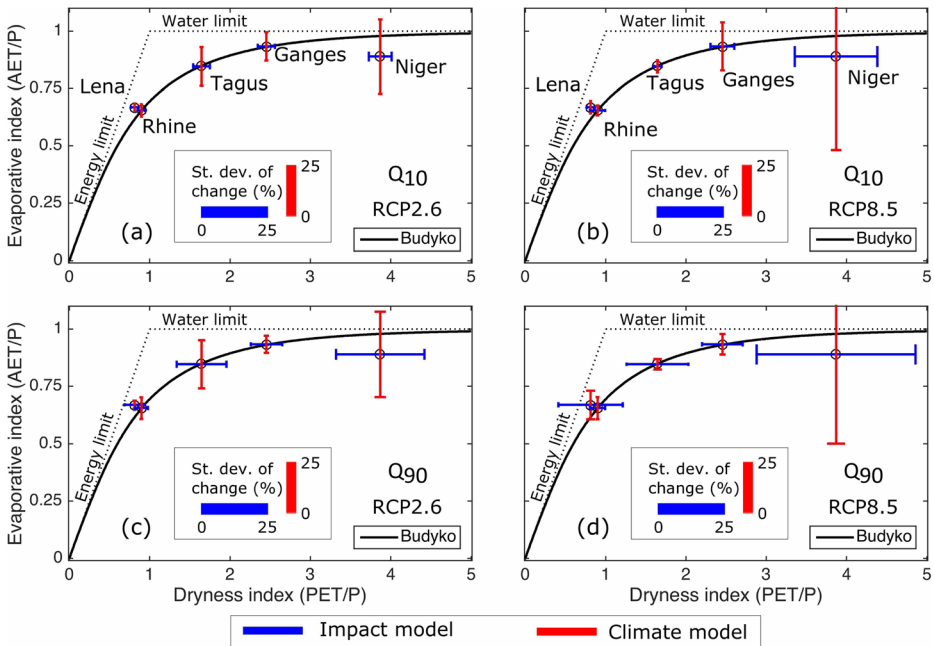
Fig. 5 Decomposition of Q_{10} (**a-b**) and Q_{90} (**c-d**) projected uncertainty into climate- (*red lines*) and impact- (*blue lines*) model propagated uncertainty as a function of the dryness and evaporative index (the black solid line depicts the Budyko curve). The magnitude of the standard deviation of change (*blue and red error bars*) is proportional to the scale given in the legend box

CM uncertainty is about five times higher than HM uncertainty for both RCP2.6 and 8.5; the standard deviation of Q_{10} change due to climate modelling is ~110 % for RCP8.5.

On the contrary, results for low flows generally show uncertainty from HMs being greater or close to CM uncertainty; this could also be related to the generally poor HM performance for low flows (see Huang et al., this special issue). Although both HM and CM uncertainties increase with increased emission scenario, the ratio between the HM and CM uncertainties seems to increase with decreasing dryness index for RCP8.5. Overall, although propagated uncertainty from CMs is higher (smaller or equal) than uncertainty from HMs for high (low) flows, both sources should be carefully assessed in climate change impacts studies. This needs additional caution in the regions with high dryness index due to increased uncertainty from both sources. See also an analysis of uncertainty propagation into drought characteristics by Samaniego et al. (this special issue).

4.5 Comparing with other recent studies

These new results from a consistent ensemble of regional HMs can be compared with both global scale and catchment scale studies over the same catchments; however, there exist very few comprehensive HM ensemble studies at the catchment scale. Global scale flooding studies using ensembles of HMs tend to analyse less frequent events than the high flow extremes considered here, but similar trends were shown by Dankers et al. (2014) and Hirabayashi et al. (2013) for all rivers considered here. On the other hand, Roudier et al. (2015) showed projected increases in the 10- and 100-year floods in the Tagus River which is opposite to the result shown here for Q_{10}.

Using the ISI-MIP ensemble of global HMs, Prudhomme et al. (2014) showed similar changes to low flows in the Lena, Rhine and Tagus Rivers, and similar uncertainty of impacts in the Niger and Ganges Rivers. Roudier et al. (2015) showed similar decreases in low flows for the Rhine and Tagus Rivers. More importantly, Prudhomme et al. (2014) suggested that the uncertainty in the ISI-MIP ensemble of global HMs could be reduced by improving process representation in these models, e.g. by analysing the HM performance when forced by observed climate. In our view, this corresponds to what was done in this study applying the regional-scale calibrated HMs.

The catchment-scale models used in ISI-MIP2 attempt to minimise bias in the calibration period, potentially reducing the uncertainties of future projections. This is the key difference between the regionally or locally calibrated HMs and the global (or continental scale) HMs; the latter can show considerable bias when compared to observed discharge (see article by Hattermann et al. (this special issue) and Roudier et al. (2015)). Indeed, Hattermann et al. (this special issue) showed that for the global HMs having much weaker performance in the historical period compared to the regional-scale HMs, there is a much larger spread in climate change impacts, which may lead to the conclusion that the uncertainty from calibrated models is smaller, given the assumption that model performance in today's climate is an indicator of the model's ability to react to changing climate (Le Vine 2016). This last issue is, however, still contested.

4.6 Limitations of this study

The uncertainties shown in this study are the known uncertainties coming from the emissions scenario, CMs and HMs. Uncertainties arising from the bias-correction used to link the CM output to the HM input are not considered, and may themselves be of a magnitude comparable to the CM or HM uncertainty (Hagemann et al. 2011; Eisner et al. 2012). Furthermore, the climate projections have not been dynamically downscaled and the bias-correction has been used to both correct and downscale in this case. It is also impossible to fully sample the range of possible outcomes from feasible CMs or HMs. Nevertheless the range of CMs-related uncertainty is large and accounts for a significant proportion of the known uncertainties (Hempel et al. 2013). The HM ensemble includes a wide range of hydrological modeling types covering various levels of complexity; however variability in plausible parameterisations of each model have not been considered, which could further increase the HM uncertainty shown. Here, all ensemble members are considered equally plausible. Probabilistic prediction methods applying weighting of different ensemble members have been tested, particularly regarding the CM choice (Kjellström et al. 2010), concluding that this may be possible for smaller scale studies (for example a river basin). This was tested for a HM ensemble by Roudier et al. (2015), where poorer performing HMs for the indices studied (e.g. low flows) were omitted from the ensemble for those indices.

5 Conclusions

This study focuses on the analysis of high and low flows in five large basins on three continents with different hydro-climatic characteristics. We also explored uncertainty in the future projections, as represented here by five GCMs, four RCPs, and five hydrological models, and how this can affect the results and conclusions. In particular, we found that:

- The distribution of change in the hydrological extremes varies with the hydro-climatic gradient, the climate projection, and the impact model.
- Both increasing and decreasing (statistically significant) trends in extremes are found depending on the future period and RCP (i.e. Niger and Rhine). The direction of trends is uncertain (and yet strong) for Niger. Lena shows an increase in high and low flows by most model combinations. Ganges shows an increase in high flows under RCP8.5 for the end-century. Tagus shows a decrease in high and low flows under RCP8.5 for the end-century.
- In terms of long-term means, high flows in the Ganges and Lena are generally expected to increase (up to ~100 % and ~40 % respectively), while reduction is generally shown for Tagus (up to −50 %). The pattern of changes in the Niger basin is not clear. Low flows in the Lena and Niger basins are expected to increase, while a reduction is shown for Rhine and Tagus (up to −50 % in the end-century). Results for Ganges are quite uncertain.
- Statistically significant changes in high and low flows increase with time, e.g. the end-century period. Niger shows the higher sensitivity to climate change, whilst Rhine shows the least sensitivity.
- A relationship between the hydrological extremes and precipitation is identified, which is particularly strong for the Niger basin.
- Uncertainty in impact assessment is related to both climate projections and impact models; however results show that uncertainty in high (low) flows is related more (slightly less) to the climate models compared to the hydrological models. Uncertainty (both related to climate and hydrological model) is generally higher in the dry than in the wet regions.

References

Aich V, Liersch S, Vetter T, et al. (2014) Comparing impacts of climate change on streamflow in four large African river basins. Hydrol Earth Syst Sci 18:1305–1321. doi:10.5194/hess-18-1305-2014

Aich V, Liersch S, Vetter T, et al (2015) Flood projections for the Niger River Basin under future land use and climate change. Sci Total Environ (Submitted).

Arheimer B, Lindström G (2015) Climate impact on floods – changes of high-flows in Sweden for the past and future (1911–2100). Hydrol Earth Syst Sci 19:771–784. doi:10.5194/hess-19-771-2015

Arnell NW (2011) Uncertainty in the relationship between climate forcing and hydrological response in UK catchments. Hydrol Earth Syst Sci 15:897–912. doi:10.5194/hess-15-897-2011

Blöschl G, Sivapalan M, Wagener T, et al. (2013) Runoff prediction in ungauged basins. Synthesis across processes, places and scales. Cambridge University Press, Cambridge, UK

Burn DH, Sharif M, Zhang K (2010) Detection of trends in hydrological extremes for Canadian watersheds. Hydrol Process 24:1781–1790. doi:10.1002/hyp.7625

Buytaert W, De Bièvre B (2012) Water for cities: the impact of climate change and demographic growth in the tropical Andes. Water Resour Res 48:WR011755. doi:10.1029/2011WR011755

Chen H, Xu C-Y, Guo S (2012) Comparison and evaluation of multiple GCMs, statistical downscaling and hydrological models in the study of climate change impacts on runoff. J Hydrol 434-435:36–45. doi:10.1016/j.jhydrol.2012.02.040

Chiew FHS, Teng J, Vaze J, Kirono DGC (2009) Influence of global climate model selection on runoff impact assessment. J Hydrol 379:172–180. doi:10.1016/j.jhydrol.2009.10.004

Christensen NS, Wood AW, Voisin N, et al. (2004) The effects of climate change on the hydrology and water resources of the Colorado River basin. Clim Chang 62:337–363. doi:10.1023/B:CLIM.0000013684.13621.1f

Collins M (2007) Ensembles and probabilities: a new era in the prediction of climate change. Phil Trans R Soc A 365:1957–1970. doi:10.1098/rsta.2007.2068

Dankers R, Arnell NW, Clark DB, et al. (2014) First look at changes in flood hazard in the inter-sectoral impact model intercomparison project ensemble. Proc Natl Acad Sci U S A 111:3257–3261. doi:10.1073/pnas.1302078110

Davie JCS, Falloon PD, Kahana R, et al. (2013) Comparing projections of future changes in runoff from hydrological and biome models in ISI-MIP. Earth Syst Dyn 4:359–374. doi:10.5194/esd-4-359-2013

Demirel MC, Booij MJ, Hoekstra AY (2013) Impacts of climate change on the seasonality of low flows in 134 catchments in the river Rhine basin using an ensemble of bias-corrected regional climate simulations. Hydrol Earth Syst Sci 17:4241–4257. doi:10.5194/hess-17-4241-2013

Donnelly C, Yang W, Dahné J (2014) River discharge to the Baltic Sea in a future climate. Clim Chang 122:157–170. doi:10.1007/s10584-013-0941-y

Eisner S, Voss F, Kynast E (2012) Statistical bias correction of global climate projections – consequences for large scale modeling of flood flows. Adv Geosci 31:75–82. doi:10.5194/adgeo-31-75-2012

Fowler HJ, Blenkinsop S, Tebaldi C (2007) Linking climate change modelling to impacts studies: recent advances in downscaling techniques for hydrological. Int J Climatol 27:1547–1578. doi:10.1002/joc.1556

Hagemann S, Chen C, Haerter JO, et al. (2011) Impact of a statistical bias correction on the projected hydrological changes obtained from three GCMs and two hydrology models. J Hydrometeorol 12:556–578. doi:10.1175/2011JHM1336.1

Hagemann S, Chen C, Clark DB, et al. (2013) Climate change impact on available water resources obtained using multiple global climate and hydrology models. Earth Syst Dyn 4:129–144. doi:10.5194/esd-4-129-2013

Hawkins E, Sutton R (2009) The potential to narrow uncertainty in regional climate predictions. Bull Am Meteorol Soc 90:1095–1107. doi:10.1175/2009BAMS2607.1

Hempel S, Frieler K, Warszawski L, et al. (2013) A trend-preserving bias correction - the ISI-MIP approach. Earth Syst Dyn 4:219–236. doi:10.5194/esd-4-219-2013

Hewitt CD, Griggs DJ (2004) Ensembles-based predictions of climate changes and their impacts. Eos (Washington DC) 85:566. doi:10.1029/2004EO520005

Hirabayashi Y, Mahendran R, Koirala S, et al. (2013) Global flood risk under climate change. Nat Clim Chang 3:816–821. doi:10.1038/nclimate1911

IPCC (2013) Climate change 2013: the physical basis. Contribution of working group 1 to the fifth assessment report of the IPCC. Cambridge University Press, New York

Kjellström E, Boberg F, Castro M, et al. (2010) Daily and monthly temperature and precipitation statistics as performance indicators for regional climate models. Clim Res 44:135–150. doi:10.3354/cr00932

Le Vine N (2016) Combining information from multiple flood projections in a hierarchical Bayesian framework. Water Resour Res 52:1–18. doi:10.1002/2015WR018143

Mann HB (1945) Nonparametric tests against trend. Econometrica 13:245–259

Minville M, Brissette F, Leconte R (2008) Uncertainty of the impact of climate change on the hydrology of a nordic watershed. J Hydrol 358:70–83. doi:10.1016/j.jhydrol.2008.05.033

Poulin A, Brissette F, Leconte R, et al. (2011) Uncertainty of hydrological modelling in climate change impact studies in a Canadian, snow-dominated river basin. J Hydrol 409:626–636. doi:10.1016/j.jhydrol.2011.08.057

Preston BL, Jones RN (2008) Evaluating sources of uncertainty in Australian runoff projections. Adv Water Resour 31:758–775. doi:10.1016/j.advwatres.2008.01.006

Prudhomme C, Giuntoli I, Robinson EL, et al. (2014) Hydrological droughts in the twenty-first century, hotspots and uncertainties from a global multimodel ensemble experiment. Proc Natl Acad Sci U S A 111:3262–3267. doi:10.1073/pnas.1222473110

Refsgaard JC, Storm B, Clausen T (2010) Système Hydrologique Europeén (SHE): review and perspectives after 30 years development in distributed physically-based hydrological modelling. Hydrol Res 41:355–377. doi:10.2166/nh.2010.009

Roudier P, Andersson JCM, Donnelly C, et al. (2015) Projections of future floods and hydrological droughts in Europe under a + 2 °C global warming. Clim Chang 135:341–355. doi:10.1007/s10584-015-1570-4

Sen PK (1968) Estimates of the regression co- efficient based on Kendall's tau. J Am Stat Assoc 63:1379–1389

Taye MT, Ntegeka V, Ogiramoi NP, Willems P (2011) Assessment of climate change impact on hydrological extremes in two source regions of the Nile River basin. Hydrol Earth Syst Sci 15:209–222. doi:10.5194/hess-15-209-2011

Teutschbein C, Seibert J (2012) Bias correction of regional climate model simulations for hydrological climate-change impact studies: review and evaluation of different methods. J Hydrol 456-457:12–29. doi:10.1016/j.jhydrol.2012.05.052

Todd MC, Taylor RG, Osborn TJ, et al. (2011) Uncertainty in climate change impacts on basin-scale freshwater resources - preface to the special issue: the QUEST-GSI methodology and synthesis of results. Hydrol Earth Syst Sci 15:1035–1046. doi:10.5194/hess-15-1035-2011

Velázquez JA, Schmid J, Ricard S, et al. (2013) An ensemble approach to assess hydrological models' contribution to uncertainties in the analysis of climate change impact on water resources. Hydrol Earth Syst Sci 17:565–578. doi:10.5194/hess-17-565-2013

Vetter T, Huang S, Aich V, et al. (2015) Multi-model climate impact assessment and intercomparison for three large-scale river basins on three continents. Earth Syst Dyn 6:17–43. doi:10.5194/esd-6-17-2015

Viviroli D, Archer DR, Buytaert W, et al. (2011) Climate change and mountain water resources: overview and recommendations for research, management and policy. Hydrol Earth Syst Sci 15:471–504. doi:10.5194/hess-15-471-2011

Weedon GP, Gomes S, Viterbo P, et al. (2011) Creation of the WATCH forcing data and its use to assess global and regional reference crop evaporation over land during the twentieth century. J Hydrometeorol 12:823–848. doi:10.1175/2011JHM1369.1